A Study on Ferroresonance Mitigation Techniques for Power Transformer

S. I. Kim, B. C. Sung, S. N. Kim, Y. C. Choi, H. J. Kim

Abstract--**This paper presents a comprehensive study on the ferroresonance mitigation techniques for a power transformer by performing four feasible solutions as follows: (a) an increase of capacity of shunt capacitance at the transformer primary side (b) a change of the transformer saturation characteristics with the low flux density (c) an insertion of the capacitor bank at the transformer secondary side (d) an installation of the resistive load bank at the transformer secondary side. In order to verify the methods mentioned above, the EMTP-RV (Electromagnetic Transients Program – Restructured Version) software is used to model the each study cases. This paper also introduces some reviews on isolating a power transformer using a disconnector, investigating the operation of surge arresters against ferroresonance overvoltage, and examining the variation of the residual flux of the iron core in a power transformer.**

***Keywords*: ferroresonance, mitigation technique, power transformer, EMTP-RV.**

I. Introduction

FERRORESONANCE is a non-linear resonance phenomenon which can be caused in a low loss electric circuit containing non-linear inductance, capacitance, and a voltage source. Non-linear inductance consists of power transformers, inductive voltage transformers and so on. Capacitance is made of cables, long transmission lines, power transformers, and grading capacitors in circuit breakers.

Contrary to inductive voltage transformers, the failure of power transformers due to ferroresonance overvoltages has not yet reported [1]. The sustained overvoltage under ferroresonance, however, can accelerate the deterioration of the insulation materials in power transformers and result in the failure of surge arresters. In order to avoid unexpected equipment damages, the effective and practical techniques should be studied.

An extensive literature on ferroresonance provides a number of countermeasures against ferroresonance in power transformers. Among these measures, four feasible solutions are examined in order to prevent the actual ferroresonance for the 25 MVA 380 / 13.8 kV YNyn0 auxiliary power transformer which is presented in Chapter II. This paper also introduces some reviews on isolating a power transformer from the grid during ferroresonance using a disconnector between them, investigating the effectiveness of the surge arresters for the actual ferroresonance, and examining the variation of the residual flux of the iron core in a power transformer.

S. I. Kim, B. C. Sung, S. N. Kim, Y. C. Choi, and H. J. Kim are with Hyundai Heavy Industries Co., Ltd., Korea (e-mail: sikim@hhi.co.kr).

Paper submitted to the International Conference on Power Systems Transients (IPST2015) in Cavtat, Croatia June 15-18, 2015

II. Ferroresonance of Power Transformer with Circuit Breaker Grading Capacitors

A ferroresonance phenomenon was experienced during a normal operation of the auxiliary power transformer bay in the 380 kV substation. The single line diagram of the 380 kV circuit to the 380 / 13.8 kV auxiliary power transformer is shown in Fig. 1 where the power transformer is connected to GIS (Gas Insulated Switchgear) via XLPE (Cross-Linked Polyethylene) cables.

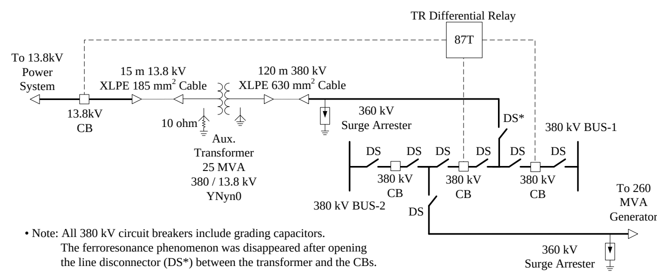

Fig. 1. Single line diagram of 380 kV circuit to 380 / 13.8 kV transformer.

The ferroresonance phenomenon was caused by an abnormal operation of the differential relay for the power transformer protection during the normal operation. Due to the sudden operation of the circuit breakers, the above 380 kV circuit is changed to a series non-linear resonance circuit with magnetizing inductance (L_{non}) of the power transformer, branch capacitance (C_b) of the cable and the power transformer, series capacitance (C_s) of the two parallel grading capacitors in circuit breakers, and resistance (R) of the load. Despite opening the circuit breakers, the series non-linear resonance circuit was energized through the grading capacitors, which operates as a source in the circuit.

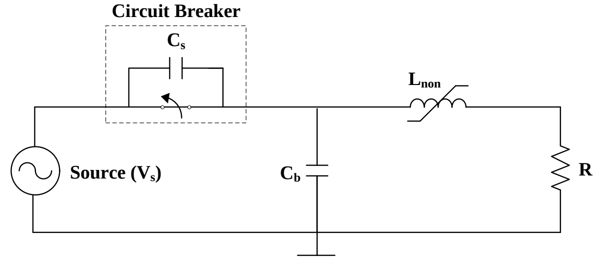

Fig. 2. Series non-linear resonance circuit.

Very loud humming sound with overvoltage and over exciting current (over flux) was detected during the ferroresonance phenomenon. The ferroresonance phenomenon was disappeared after opening the line disconnector (DS* of Fig. 1) between the transformer and the circuit breakers. The distorted voltage waveforms with amplitude of 1.28 ~ 1.55 pu and over exciting current waveforms were recorded.

In order to simulate the ferroresonance phenomenon and find its countermeasures, the circuit of the 380 kV substation is modeled using the EMTP-RV software. The on-site parameters and estimated data for the 380 kV substation are applied to this model.

The simulation model consists of a source, a series capacitor, a branch capacitor, a non-linear inductor, and a resistor. The source voltage is 395 kV (1.04 pu) and the source impedance is not considered due to the lack of data. Grading capacitors in the circuit breakers and phase-to-ground capacitance of the power system components are modeled as the combination of the series capacitor and the branch capacitor. To implement the saturation characteristics of the transformer more precisely, the BCTRAN transformer model [2] with an externally attached core is used (Fig. 3).

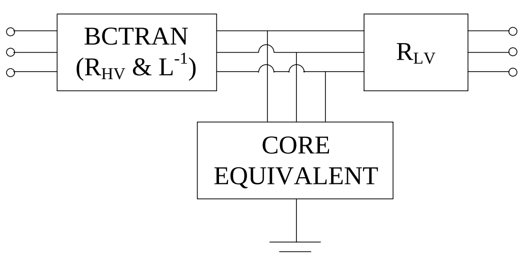

Fig. 3. BCTRAN transformer model with externally attached core [3].

It is made of winding resistance, leakage inductance, magnetizing resistance, and non-linear magnetizing inductance. The winding resistance and leakage inductance are calculated by short-circuit test data of the transformer. The magnetizing resistance and non-linear magnetizing inductance are calculated by using no-load test data of the transformer. The load is modeled by a pure resistor.

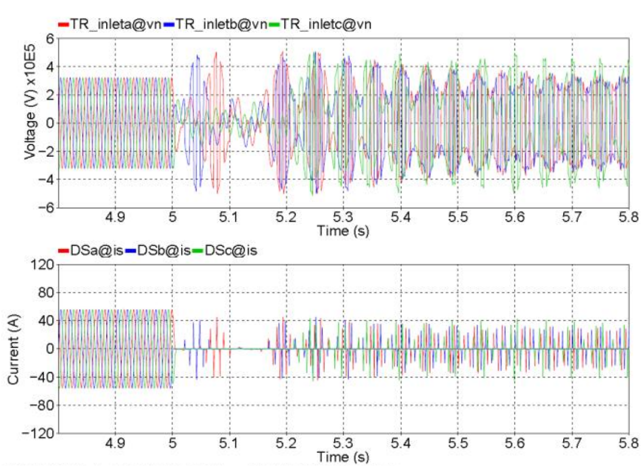

Fig. 4. Voltages at transformer primary side (upper) and line currents (lower) for simulation model.

When the transformer is de-energized by opening the HV side circuit breakers at 0.5 sec, the LV side circuit breaker is also opened at the same time and there is no load on the secondary side of the transformer. The voltages at the transformer primary side and line currents are shown in Fig. 4.

III. Mitigation Techniques

According to CIGRE technical brochure no. 569, mitigation techniques applicable to the power transformer are grouped into three basic approaches [1]:

- Avoid circuit parameters or operating conditions favouring ferroresonance
- Minimize the energy transfer that is required to sustain the ferroresonant oscillations
- Control the duration of ferroresonance by the operational switching

Based on these approaches, four kinds of the mitigation techniques are derived as follows: (a) an increase of the capacity of shunt capacitance at the transformer primary side (b) a change of the transformer saturation characteristics with the low flux density (c) an insertion of the capacitor bank at the transformer secondary side (d) an installation of the resistive load bank at the transformer secondary side.

A. *Shunt capacitance at HV side*

The first solution is to place additional shunt capacitance between the transformer and the GIS. To analyze the effect of the shunt capacitance easily, the series non-linear resonance circuit shown in Fig. 2 can be converted into the equivalent circuit of Fig. 5 [4].

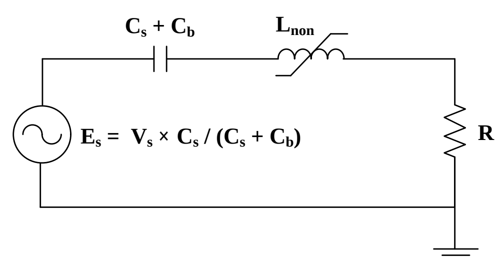

Fig. 5. Equivalent circuit of series non-linear resonance circuit

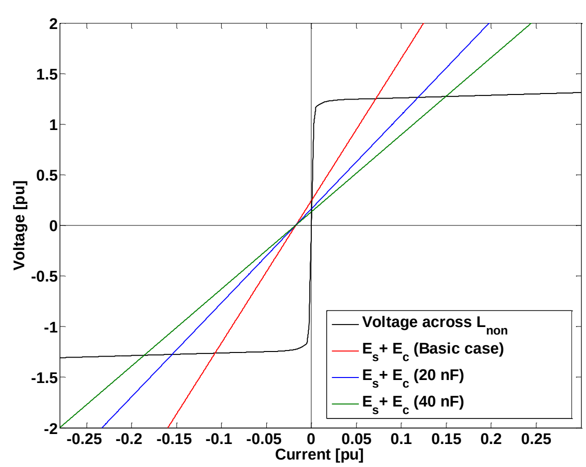

Fig. 6. Effect of increasing shunt capacitance

The effect of the shunt capacitance is shown in Fig. 6. The higher capacitance results in a reduced slop of the "E_s + E_c" line where E_s is the equivalent source voltage and E_c is the voltage across the capacitance "C_s + C_b". As the source voltage decreases, the "E_s + E_c" line moves downwards. Intuitively, the graphical solution shows that the higher capacitance helps to reduce the risk of ferroresonance.

In order to confirm its effectiveness, the ferroresonance study when 20 nF and 40 nF of capacitors are installed at the transformer primary side is conducted. The simulation results are summarized in Table I, and Fig. 7 shows voltage waveforms at transformer primary side for case 1 and case 2.

Industry analysts have empirically assumed that when the voltage exceeds 1.25 pu, the system is said to be "in ferroresonance" [5]. According to this concept, ferroresonance can be avoided by installing the 40 nF of capacitor in this study.

TABLE I
SIMULATION RESULTS OF MAXIMUM OVERVOLTAGE FOR SHUNT CAPACITORS

Cases	Capacitor	Maximum overvoltage	State
Case 1	20 nF	1.50 pu	In ferroresonance
Case 2	40 nF	0.78 pu	Non ferroresonance

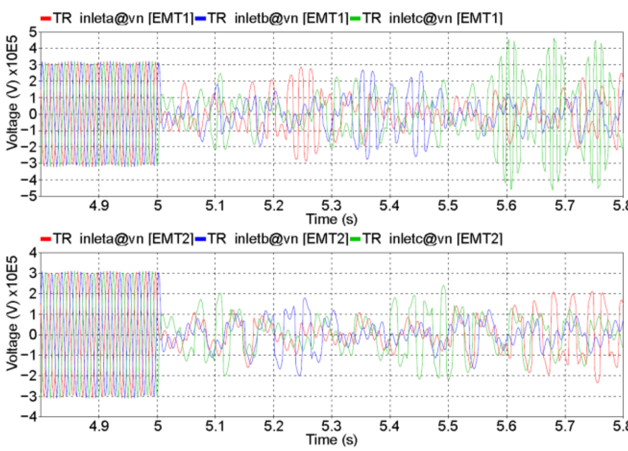

Fig. 7. Voltages at transformer primary side for Case 1 (upper) and Case 2 (lower).

The additional shunt capacitance connected in the transformer primary side is very effective to reduce the risk of ferroresonance. Despite the high cost of implementation, it is one of the best solutions if the transformer secondary side is not accessible.

B. Transformer Saturation

The second solution is to specify the transformers with the lower flux density by increasing the cross section area of the iron core in the transformer. Most of the power transformers are designed to have approximately 1.2 pu of the saturation voltage (basic case, presented in Fig. 4) due to the economic reasons. In this study, the ferroresonance analysis for the 380 kV substation containing the transformer with the lower flux density, which has approximately 1.4 pu of the saturation voltage, is carried out to review the effect of the transformer saturation characteristics. The magnetizing curve of the transformer with the normal and lower flux density applied to this study is shown in Fig. 8.

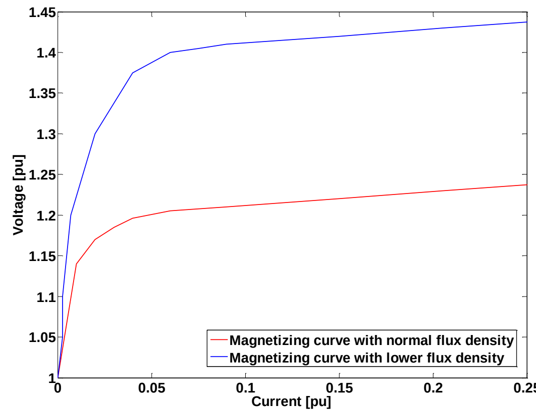

Fig. 8. Magnetizing curve of power transformer

Fig. 9 shows voltage waveforms at the transformer primary side and line currents for the transformer with the low flux density. After opening the HV side circuit breakers, the distorted voltage waveforms with the low frequency component are observed at the initial stage of the simulation and these lead to ferroresonance eventually.

As shown in the upper one of Fig. 9, since the frequency of the voltage is decreased drastically after the operation of the circuit breaker, it contains a small amount of DC component. This DC component of the transformer terminal voltage may saturate the core of the transformer in spite of its increased saturation characteristic. Therefore, the solution is turned out to be neither practical nor economical.

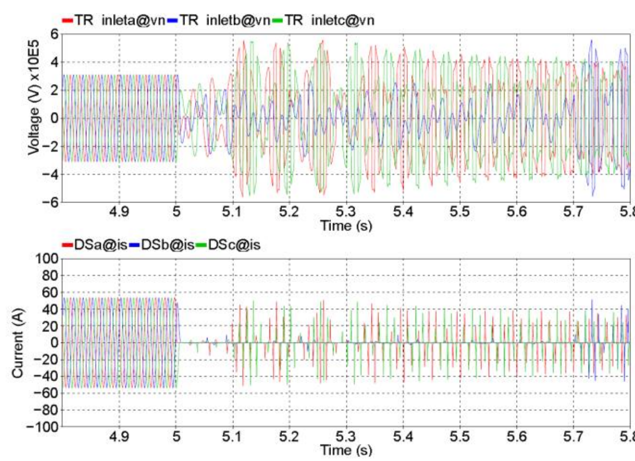

Fig. 9. Voltages at transformer primary side (upper) and line currents (lower) for transformer saturation.

C. Capacitor Bank at LV side

The third solution is to install the capacitor bank to suppress ferroresonance. As many papers and technical reports propose the insertion of the capacitor bank at the delta connected tertiary winding [6]. This can only be applicable to the power transformers with tertiary winding terminals. It is considered that the capacitor bank is located at the transformer secondary side in the study because the transformer applied to this study does not have tertiary winding.

In the simulation, the capacitor banks are increased from 2 % to 20 % (0.5 MVar ~ 5 MVar) of the capacity of the transformer. The simulation results are summarized in Table II. Voltage waveforms for Case 1, Case 2, Case 3, and Case 4 are presented in Fig. 10 and Fig. 11 to understand the effect of the capacitor bank clearly.

TABLE II
SIMULATION RESULTS OF MAXIMUM OVERVOLTAGE FOR CAPACITOR BANKS

Cases	Capacitor bank capacity	Maximum overvoltage	State
Case 1	5.0 MVar	0.27 pu	Non ferroresonance
Case 2	3.0 MVar	0.41 pu	Non ferroresonance
Case 3	1.0 MVar	0.87 pu	Non ferroresonance
Case 4	0.5 MVar	1.87 pu	In ferroresonance

Fig. 10 shows voltage waveforms at the transformer primary side when the transformer is connected to 12 % and 20 % of the capacitor bank. It can be observed that the high capacity of the capacitor bank is very effective on the suppression of ferroresonance.

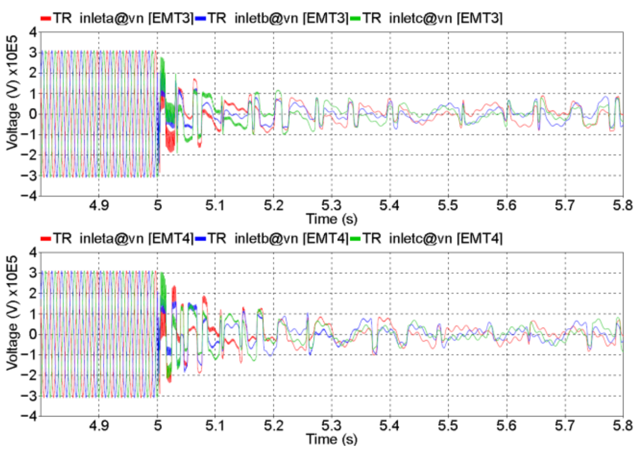

Fig. 10. Voltages at transformer primary side for Case 1 (upper) and Case 2 (lower).

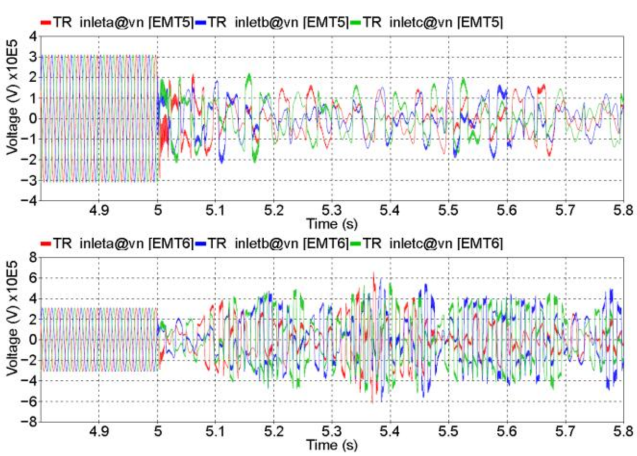

Fig. 11. Voltages at transformer primary side for Case 3 (upper) and Case 4 (lower).

Fig. 11 shows voltage waveforms at transformer primary side when the transformer is connected to 2 % and 4 % of the capacitor bank. Ferroresonance can be avoided by installing the capacitor bank with the capacity of 4 % of its capacity.

This countermeasure has the disadvantages such as its higher cost and the possibility of explosion in practice. In other words, the capacitor bank at the transformer secondary side can significantly reduce the risk of ferroresonance, however it also has disadvantages as well.

D. Resistive Load Bank at LV Side

The last solution is to place the suitable resistive load bank to the transformer secondary side. It increases the loss of the series non-linear resonance circuit. Fig. 12 shows the graphical solution of the series non-linear resonance circuit without the resistor for the basic case where P_1 is a non-ferroresonant stable operation point, P_2 is an unstable operating point, and P_3 is a ferroresonant stable point [7]. In case of the circuit without the resistance, there are three intersection points with "$|E_L$ - $E_c|$" line and "Es" line which contains a ferroresonant stable point (P_3). Thus, the ferroresonance phenomenon can occur in this condition.

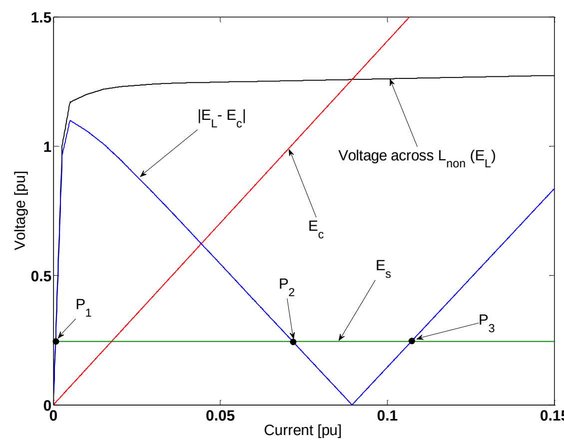

Fig. 12. Graphical solution of series non-linear ferroresonance circuit without resistance [7].

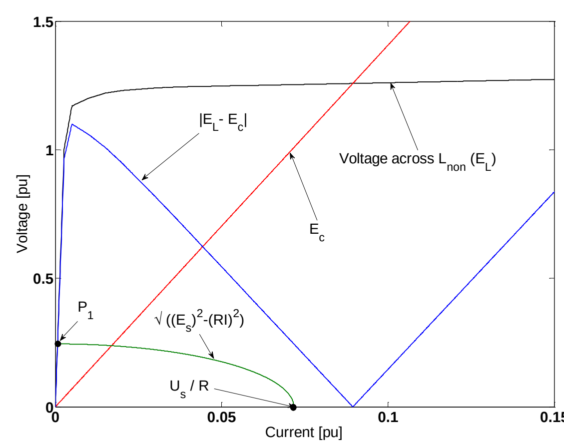

Fig. 13. Graphical solution of series non-linear ferroresonance circuit with resistance [1].

Fig. 13 shows the graphical solution of the circuit with the resistance. If the high capacity of the resistive load bank is connected, there is only one intersection point with "$|E_L - E_c|$" line and "$((E_s)^2-(RI)^2)^{1/2}$" line which corresponds to a non-ferroresonant stable operation point. This describes that the occurrence of ferroresonance can be avoided by introducing the resistive load bank [1].

In the simulation, the resistive load banks are increased from 0.4 % to 4 % (0.1 MW ~ 1 MW) of the transformer to find the proper capacity for the ferroresonance suppression. The simulation results are summarized in Table III. Voltage waveforms for Case 1, Case 2, Case 3, and Case 4 are presented in Fig. 14 and Fig. 15.

TABLE III
SIMULATION RESULTS OF MAXIMUM OVERVOLTAGE FOR RESISTIVE LOAD BANKS

Cases	Resistive load bank capacity	Maximum overvoltage	State
Case 1	1.0 MW	0.23 pu	Non ferroresonance
Case 2	0.5 MW	0.39 pu	Non ferroresonance
Case 3	0.3 MW	0.44 pu	Non ferroresonance
Case 4	0.1 MW	1.47 pu	In ferroresonance

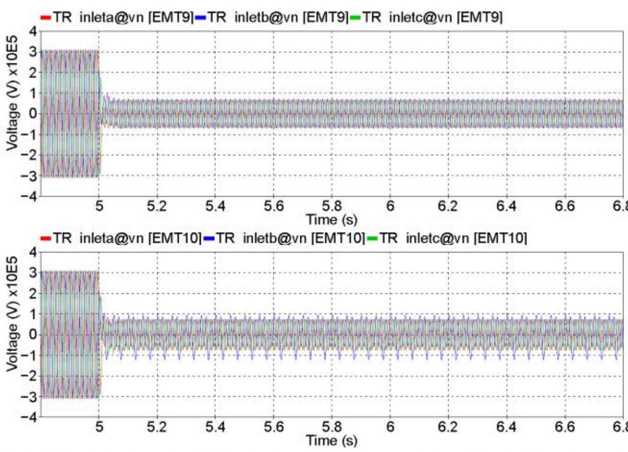

Fig. 14. Voltages at transformer primary side for Case 1 (upper) and Case 2 (lower).

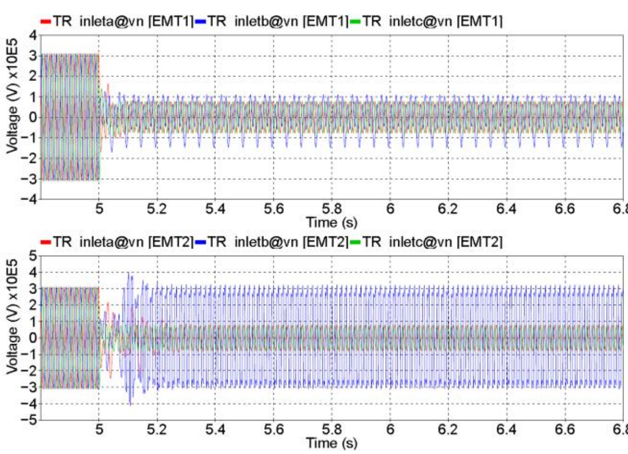

Fig. 15. Voltages at transformer primary side for Case 3 (upper) and Case 4 (lower).

Fig. 14 and Fig. 15 show the voltage waveforms at the transformer primary side when the transformer is connected to 0.4 %, 1.2 %, 2 %, and 4 % of the resistive load bank. The maximum overvoltage is reduced as the resistive load banks are increased. It is also observed that the resistive load bank with 1.2 % of the transformer capacity can mitigate the magnitude of the maximum overvoltage below 1.25 pu.

This countermeasure is cheaper and smaller size than the capacitor bank, and consequently the installation of the resistive load bank is turned out to be one of the effective methods. As a matter of fact, this method is still expensive and takes up so much space because medium voltage switchgears (including vacuum circuit breaker, current transformer, protective relay, and local control cabinet) and ventilation facilities with an air duct have to be installed additionally.

IV. ADDITIONAL REVIEW

There are some issues on ferroresonance as follows:

- Isolating a power transformer from the grid during ferroresonance oscillations using a disconnector between the transformer and the circuit breaker
- Effectiveness of surge arresters for the actual ferroresonance
- Varying residual flux of the iron core in a power transformer

A. *Opening disconnector*

Isolating a power transformer from the grid during opening a disconnector is one of the possible countermeasures. Generally, disconnectors are used to ensure the de-energization of electrical circuits. The disconnectors can interrupt only low levels of capacitive current or small inductive current. Thus, it raises a question about whether the disconnectors are able to open the over exciting current due to ferroresonance without any damage to their contacts.

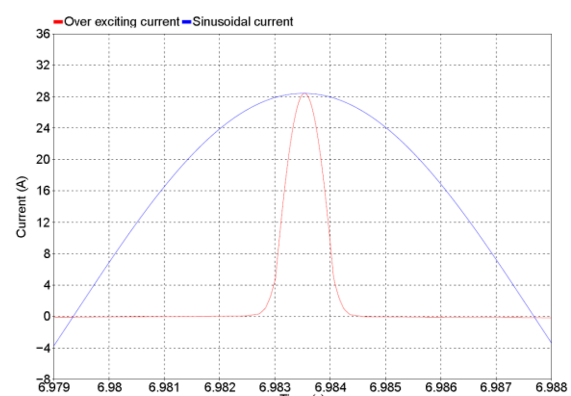

Fig. 16. Enlarged view of over exciting current for basic case together with the sinusoidal current

An enlarged view of the over exciting current for the basic case together with the sinusoidal current is shown in Fig. 16. It is possible to observe the distorted waveforms of the over exciting current. Differences in their waveforms make it difficult to compare the interrupting capability of disconnectors for the over exciting current. However, it can be inferred from Fig. 16 that even if the amplitude of the over exciting current is higher than the capability of disconnectors, disconnectors can interrupt the over exciting current due to its short-duration peak current.

The actual ferroresonance for the 380 kV substation described in Chapter II can be disappeared by opening the disconnector without the damage to their contacts. It might have been that the disconnector operated at the low current.

In the 230 kV substation, the failure of disconnector contacts due to large arcing during interrupting the ferroresonant current has been reported recently. It resulted in flashover in the 230 kV GIS.

Opening disconnector is the easiest way of reducing ferroresonance. However, extra attention must be paid to suppress the ferroresonance because a normal disconnector is capable of disconnecting only small amount of current. Therefore, further research is needed for disconnestor's interrupting capacity of ferroresonant current.

B. *Surge arrester operation*

In case of the actual ferroresonance, the surge arresters installed at the 380 kV substation did not operate for the ferroresonance overvoltage. It can be checked through whether the counters of the surge arresters operated or not.

In order to review the surge arrester operation during ferroresonance, the typical voltage – current characteristics of the 360 kV surge arrester installed at the 380 kV substation are examined and shown in Fig. 17 and Table IV.

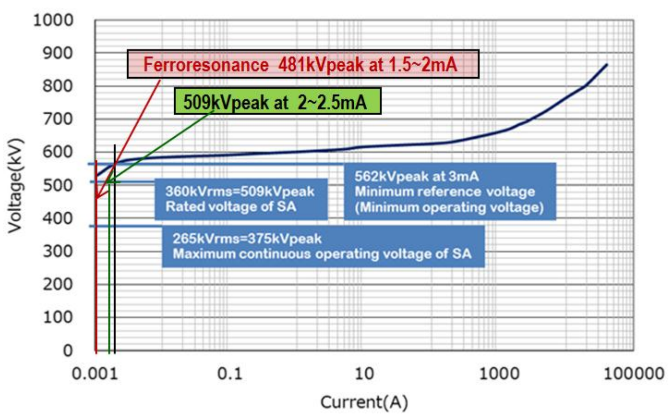

Fig. 17. Typical V-I characteristics of 360 kV surge arrester.

TABLE IV
TECHNICAL DATA OF 360 KV SURGE ARRESTER

Technical Data	Value
Rated voltage	509 kV_{peak} at 2 ~ 2.5 mA_{peak}
Min. operating voltage and current	562 kV_{peak} at 3 mA_{peak}
Max. cont. operating voltage & current	375 kV_{peak} at 1 ~ 2 mA_{peak}

Fig. 17 and Table IV show that the 360 kV surge arresters cannot operate for the maximum ferroresonance overvoltage with amplitude of 1.55 pu. The result of this review corresponds to the IEC standard [8]. It states that the temporary overvoltages due to ferroresonance should not form the basis to select the surge arrester. The use of a surge arrester as an extra burden to reduce the ferroresonance is not effective and unproven.

If very high overvoltage results from ferroresonance, the surge arrester would work for that. Without the rapid action of on-site engineer to eliminate ferroresonance, the sustained overvoltage can result in the failure of surge arresters.

C. *Residual flux*

The important factors of ferroresonance occurrence are initial charge on the capacitors, the residual flux in the core of the transformers, and switching instant [9]. Among these factors, the residual flux is the most important because it can drive the iron core into heavy saturation. This is the reason for examining the variation of the residual flux.

This study investigates the variation of the residual flux of the iron core in the power transformer, which depends on both the opening instant of disconnectors and the duration of ferroresonance.

After the disconnector is interrupted by different voltage phase at 0, $\pi/2$, π, and $3\pi/2$ radians, respectively, the amplitudes of the residual flux are calculated. Fig 18 shows that the switching instant has no effect on the variation of the residual flux.

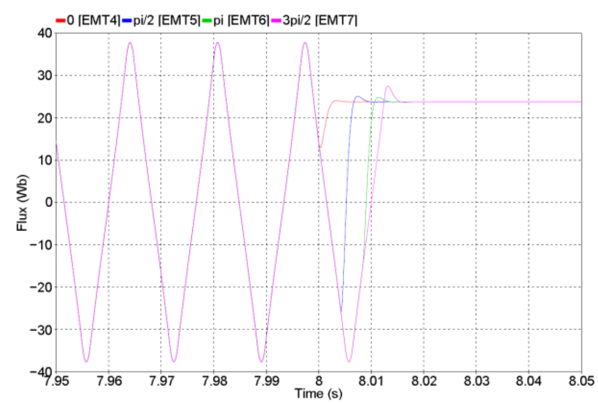

Fig. 18. Variation of residual flux depending on opening instant (Switching instant: red-0, blue- $\pi/2$, green-π, pink- $3\pi/2$).

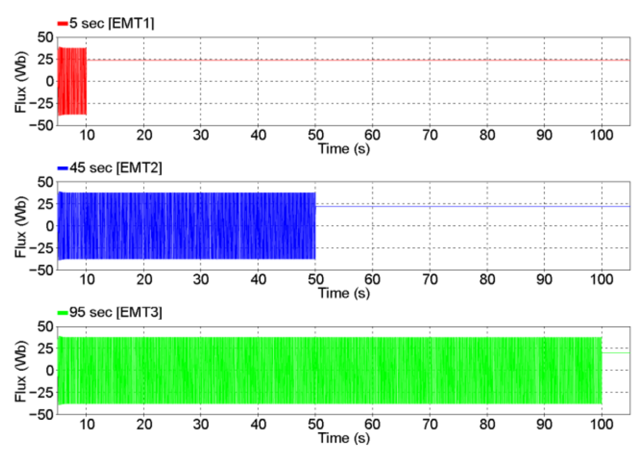

Fig. 19. Variation of residual flux depending on duration time (Top: 5 sec – 23.7 Wb·t, Middle: 45 sec – 22.1 Wb·t, Bottom: 95 sec – 20.2 Wb·t).

The residual flux is also examined after the durations of ferroresonance for 5 sec, 45 sec, and 95 sec. From Fig. 19, it is found that the amplitudes of the residual flux decrease continuously in accordance with prolonging the ferroresonance.

V. CONCLUSIONS

This paper presents not only a study on the ferroresonance mitigation techniques for a power transformer but also some reviews on a ferroresonance phenomenon. From the study results, the effective methods are to increase the shunt capacitance at the transformer primary or secondary side and to install the suitable resistive load bank. However, there are also disadvantages in the costs and spaces. Therefore, the design engineers of substation have to take a close review for the occurrence of ferroresonance at the design stage.

VI. REFERENCES

[1] CIGRE Working Group C4.307, "Resonance and ferroresonance in power networks," CIGRE, Tech. Bro. TB-569, Feb. 2014.

[2] V. Brandwajn, H. W. Dommel, and I. I. Dommel, "Matrix representation of three-phase n-winding transformers for steady-state and transient studies," *IEEE Trans. Power App. Syst.*, vol. 1, pp. 1369-1378, June 1982.

[3] CIGRE Working Group C4.307, "Transformer energization in power systems: a study guide," CIGRE, Tech. Bro. TB-568, Feb. 2014.

[4] D. A. N. Jacobson, "Field testing, modelling and analysis of ferroresonance in a high voltage power system," Ph.D. dissertation, Dept. Elec. and Com. Eng., Univ. Manitoba, Winnipeg, 2000.

[5] S. Santoso, R. C. Dugan, and P. Nedwick, "Modeling ferroresonance phenomena in an underground distribution system," in *Proc. 2001 IPST*.

[6] A. V. Ranst, J. M. Dumoulin, and N. Mabrouk, "Insulation coordination and ferro-resonance study for EMAL phase II project," Tractebel Eng., Brussels, BE, Apr. 2012.

[7] V. Valverde, A. J. Mazon, I. Zamora, and G. buigues, "Ferroresonance in voltage transformers: analysis and simulations," in *Proc. 2007 ICREPQ*.

[8] *IEC Standard for Surge arresters – Part5: Selection and application recommendations*, IEC Standard 60099-5 ed2.0, Mar. 2013.

[9] P. Ferracci, "Ferroresonance," Schneider Electric Corp., Cahier Technique N-190, Mar. 1998.